Title

Pan-viral serology implicates enteroviruses in acute flaccid myelitis

Journal

Nature Medicine, 25(11)

ISSN

1078-8956

Authors

Schubert, Ryan D

Hawes, Isobel A

Ramachandran, Prashanth S

et al.

Publication Date

2019-11-01

DOI

10.1038/s41591-019-0613-1

Peer reviewed

HHS Public Access

Author manuscript

Nat Med. Author manuscript; available in PMC 2020 April 21.

Published in final edited form as:

Nat Med. 2019 November ; 25(11): 1748–1752. doi:10.1038/s41591-019-0613-1.

Pan-viral serology implicates enteroviruses in acute flaccid myelitis

Ryan D. Schubert, MD[1,2], **Isobel A. Hawes, BS**[1,*], **Prashanth S. Ramachandran, MBBS**[1,2,*], **Akshaya Ramesh, PhD**[1,2,*], **Emily D. Crawford, PhD**[3,4], **John E. Pak, PhD**[3], **Wesley Wu, PhD**[3], **Carly K. Cheung, BS**[3], **Brian D. O'Donovan, PhD**[5], **Cristina M. Tato, PhD**[3], **Amy Lyden, BS**[3], **Michelle Tan, BS**[3], **Rene Sit, BA**[3], **Gavin A. Sowa, BS**[6], **Hannah A. Sample, BS**[5], **Kelsey C. Zorn, MHS**[5], **Debarko Banerji, BS**[2], **Lillian M. Khan, BS**[5], **Riley Bove, MD**[1,2], **Stephen L. Hauser, MD**[1,2], **Amy A. Gelfand, MD, MAS**[1], **Bethany Johnson-Kerner, MD, PhD**[1,2], **Kendall Nash, MD**[1], **Kalpathy S. Krishnamoorthy, MD**[7], **Tanuja Chitnis, MD**[7,8], **Joy Z. Ding, MD**[9], **Hugh J. McMillan, MD, MSc**[9], **Charles Y. Chiu, MD, PhD**[10], **Benjamin Briggs, MD, PhD**[11], **Carol A. Glaser, DVM, MPVM, MD**[12], **Cynthia Yen, MPH**[13], **Victoria Chu, MD, MPH**[13], **Debra A. Wadford, PhD**[13], **Samuel R. Dominguez, MD, PhD**[14], **Terry Fei Fan Ng, PhD**[15], **Rachel L. Marine, PhD**[15], **Adriana S. Lopez, MHS**[15], **W. Allan Nix, BS**[15], **Ariane Soldatos, MD, MPH**[16], **Mark P. Gorman, MD**[17], **Leslie Benson, MD**[17], **Kevin Messacar, MD**[14], **Jennifer L. Konopka-Anstadt, PhD**[15], **M. Steven Oberste, PhD**[15], **Joseph L. DeRisi, PhD**[3,5], **Michael R. Wilson, MD, MAS**[1,2,**]

[1]UCSF Weill Institute for Neurosciences, San Francisco, CA, USA

[2]UCSF Department of Neurology, San Francisco, CA, USA

[3]Chan Zuckerberg Biohub, San Francisco, CA, USA

[4]UCSF Department of Microbiology and Immunology, San Francisco, CA, USA

[5]UCSF Department of Biochemistry & Biophysics, San Francisco, CA, USA

**Corresponding Author Information: Name: Dr. Michael Wilson, Address: UCSF, Department of Neurology, Division of Neuroimmunology and Glial Biology, 675 Nelson Rising Lane, NS212, Campus Box 3206, San Francisco, CA 94158, michael.wilson@ucsf.edu, Phone: 415-502-7429.

Author Contributions

A.R. computationally designed the VirScan peptide library. R.D.S., I.A.H., and G.A.S. cloned the VirScan library. R.D.S. and I.A.H. performed the VirScan experiments. R.D.S. and B.O. developed the automated IP protocols and analysis pipeline for VirScan. J.E.P., W.W., and C.K.C. cloned and expressed enterovirus VP1 proteins. R.D.S. performed the ELISA experiments. P.S.R., E.D.C., A.L., C.M.T., M.T., and R.D.S. performed metagenomic sequencing and FLASH. P.S.R. and E.D.C. analyzed metagenomic and FLASH data. D.B. and L.M.K. helped prepare samples for sequencing. R.D.S., H.A.S., K.C.Z., R.B., S.L.H., A.A.G., B.J.K., K.N., K.S.K., T.C., J.Z.D., H.J.M., C.Y.C., B.B., C.A.G., C.Y., V.C., D.A.W., S.R.D., R.L.M., A.S.L., W.A.N., A.S., M.P.G., L.B., K.M., J.L.K-A, and M.S.O. identified patients, performed clinical phenotyping and provided patient samples. R.D.S., A.R., T.F.F.N., J.L.D., and M.R.W. analyzed VirScan and ELISA data. R.D.S. and J.L.D. generated the figures. J.L.K-A and M.S.O. provided critical expert guidance on the manuscript. R.D.S., J.L.D., and M.R.W. conceived of and wrote the manuscript. All authors discussed the results and contributed critical review to the manuscript.

*Authors contributed equally

Competing Interests Statement

The authors have no competing interests to declare.

Publisher's Disclaimer: Disclaimer

The findings and conclusions in this report are those of the author(s) and do not necessarily represent the official position of the Centers for Disease Control and Prevention, the National Institutes of Health or the California Department of Public Health.

[6]UCSF School of Medicine, San Francisco, CA, USA

[7]Department of Neurology, Massachusetts General Hospital, Boston, MA, USA

[8]Department of Neurology, Brigham and Women's Hospital, Boston, MA, USA

[9]Division of Neurology, Children's Hospital of Eastern Ontario, University of Ottawa, Ottawa, Ontario, Canada.

[10]Department of Laboratory Medicine and Medicine, Division of Infectious Diseases, University of California, San Francisco, San Francisco, USA

[11]Department of Pediatrics, Division of Infectious Diseases, University of California, San Francisco, San Francisco, USA

[12]Department of Pediatric Infectious Diseases, Kaiser Permanente Oakland Medical Center, Oakland, California, USA

[13]Division of Communicable Disease Control, California Department of Public Health, Richmond, California

[14]Children's Hospital Colorado and Department of Pediatrics, University of Colorado School of Medicine, Aurora, CO, USA.

[15]Division of Viral Diseases, Centers for Disease Control and Prevention, Atlanta, GA, USA

[16]National Institute of Neurological Disorders and Stroke (NINDS), NIH, Bethesda, Maryland, USA.

[17]Department of Neurology, Boston Children's Hospital, Boston, MA, USA

Abstract

Since 2012, the United States has experienced a biennial spike in pediatric acute flaccid myelitis (AFM).[1–6] Epidemiologic evidence suggests non-polio enteroviruses (EVs) are a potential etiology, yet EV RNA is rarely detected in cerebrospinal fluid (CSF).[2] We interrogated CSF from children with AFM (n=42) and pediatric other neurologic disease controls (n=58) for intrathecal anti-viral antibodies using a phage display library expressing 481,966 overlapping peptides derived from all known vertebrate and arboviruses (VirScan). We also performed metagenomic next-generation sequencing (mNGS) of AFM CSF RNA (n=20 cases), both unbiased and with targeted enrichment for EVs. Using VirScan, the only viral family significantly enriched by the CSF of AFM cases relative to controls was *Picornaviridae*, with the most enriched *Picornaviridae* peptides belonging to the genus *Enterovirus* (n=29/42 cases versus 4/58 controls). EV VP1 ELISA confirmed this finding (n=22/26 cases versus 7/50 controls). mNGS did not detect additional EV RNA. Despite rare detection of EV RNA, pan-viral serology identified frequently high levels of CSF EV-specific antibodies in AFM compared to controls, providing further evidence for a causal role of non-polio EVs in AFM.

Introduction

First detected in California in 2012, the United States has experienced seasonal, biennial increases in the incidence of acute flaccid myelitis (AFM) cases.[7] Since 2014, the Centers

for Disease Control and Prevention (CDC) has reported over 500 confirmed cases.[1–4,8] The nationwide surges in AFM in 2014, 2016, and 2018 have coincided temporally and geographically with outbreaks of enterovirus (EV) D68 and EV-A71 infections.[2,6,9–11] EVs, including poliovirus, are well recognized for their neuroinvasive capacity and resultant central nervous system (CNS) pathology, ranging from self-resolving aseptic meningitis to fulminant, sometimes fatal, brainstem encephalitis, and to myelitis leading to permanent debilitating paralysis.[12]

Despite the temporal association between EV-D68 and EV-A71 outbreaks and AFM and a mouse model that recapitulates the AFM phenotype with a contemporary EV-D68 strain,[13] the etiology of AFM has been difficult to confirm.[14,15] Thus, concerns persist that AFM could result from yet-to-be-identified pathogens or a para-infectious immune response. This is due, in part, to the fact that less than half of children with AFM have had EV detected in a non-sterile biologic specimen (nasopharyngeal or oropharyngeal swabs most commonly, rectal and stool samples less commonly), and no other alternative candidate etiologic agents have been identified in the remaining children.[3] In addition, only 2% of children with AFM have EV nucleic acid detected in cerebrospinal fluid (CSF).[16,17]

The immune privileged status of the CNS makes direct detection of viral nucleic acid or indirect discovery of intrathecal anti-viral antibodies an important step in linking a pathogen to a neuroinfectious disease. We interrogated CSF from AFM patients from recent outbreaks with unbiased ultra-deep metagenomic next-generation sequencing (mNGS), including a novel CRISPR-Cas9 based enrichment technique called FLASH (Finding Low Abundance Sequences by Hybridization).[18] Furthermore, to search for virome-wide antibody signals that might be associated with AFM, we employed the VirScan approach that was previously developed to detect antibodies to all known human viruses.[19] To improve upon this detection method, we generated a large and more finely tiled peptide library in the T7 bacteriophage display vector described in detail in Methods.

Results

Cases and Controls

42 AFM cases and 58 other neurologic disease (OND) controls were included in the study (Extended Data 1). Patient demographics are described in Table 1 with detailed information on available clinical diagnostic testing in Supplemental Tables 1A and 1B. The AFM cases were younger (median age 37.8 months, interquartile range [IQR], 11 to 64 months) than the OND controls (median age 120 months, IQR, 66 to 174 months), with a p-value of 0.0497 (as determined by an unpaired parametric t-test). There was a higher proportion of males in the AFM cases. AFM cases and OND controls from the Western and Northeastern USA make up the majority of both categories. Most AFM cases were from 2018.

Ultra-Deep Metagenomic Next-Generation Sequencing Rarely Detects Enterovirus in AFM

We obtained an average of 433 million 150 nucleotide (nt) paired-end reads per sample (range, 304 – 569 million reads per sample). Based on the External RNA Controls Consortium (ERCC) RNA spike-ins, we estimated that our mean limit of detection was 5.48

attograms (range, 3.92 to 17.47 attograms).[20] EV-A71 was detected in one AFM sample at 71.31 reads per million (rpM) (1497.3 rpM in FLASH-NGS, Supplemental Tables 2 and S3). This sample was previously known to be EV-A71 positive by EV RT-PCR and Sanger sequencing. No other pathogenic organisms were detected in this or any of the other AFM samples. The non-human sequence reads from each sample were deposited at the National Center for Biotechnology Information Sequence Read Archive (PRJNA557094).

CSF VirScan Testing Detects Enterovirus Antibodies in AFM

The only significantly enriched viral family by VirScan of CSF in AFM cases (n = 42) versus OND controls (n = 58) was *Picornaviridae* (mean rpK 11,082, IQR 16,850 versus mean rpK 1121 IQR 974, p-adjusted = 6.3×10^{-8} Mann-Whitney test with Bonferroni adjustment, Supplemental Table 4). Enriched *Picornaviridae* peptides belonged almost entirely to the genus *Enterovirus* (Figure 1A–C, Supplemental Table 5), with 69% (29/42) of AFM cases versus 7% (4/58) of OND controls considered positive for EV antibodies by VirScan. Enriched EV peptides were derived from proteins across the EV genome (Figure 2A, Supplemental Table 6A). Peptides mapping to *Sapelovirus* and unclassified *Picornaviridae* were also significantly enriched in AFM relative to OND controls (p-adjusted = 0.013 and 0.00038, respectively by Mann-Whitney test with Bonferroni adjustment). Using the EV-A71 genome as a model reference EV as in Figure 2A, 99% and 95% of the rpK signal for *Sapelovirus* and unclassified *Picornaviridae* mapped to EV-A71 using BLASTP (e-value threshold 0.01, word size 2) (Supplemental Tables 6B and C).

Among capsid protein sequences, KVPALQAAEIGA in VP1 was previously reported to be an immunodominant linear EV epitope.[21,22] Peptides containing this and related overlapping epitopes were enriched in our data across AFM patients, with multiple sequence alignment revealing a consensus motif of PxLxAxExG (Figure 2B). Another immunodominant epitope was to a conserved, linear portion of 3D (Figure 2C).

Enterovirus VP1 ELISA confirms VirScan Findings

Consistent with the VirScan data, the mean EV VP1 ELISA signal in AFM (n = 26, mean OD 0.51 IQR 0.56) was significantly higher than OND controls (n = 50, mean OD 0.08 IQR 0.06, p-value < 0.001 by Mann-Whitney test, Figure 3 and per-patient data in Supplemental Tables 1A and 1B). The EV signal detected by phage and ELISA demonstrated a linear correlation ($R^2 = 0.511$, p-value < 0.001, Extended Data 2). Among AFM patients, mean CSF EV antibody levels detected by either ELISA or VirScan did not differ based on whether EV RNA had been previously detected (n =15) or not (n = 11) (mean OD 0.41 versus 0.65 by ELISA; mean rpK 6,093 vs 14,489 by VirScan, p-value = not significant for both comparisons). In total, 85% (22/26) of a subset of AFM versus 14% (7/50) of OND tested by ELISA demonstrated reactivity against VP1. ELISA confirmed 18/19 EV positive VirScan samples and identified 11 additional EV positive samples. Additional samples detected by ELISA did have EV phage signal by VirScan but were below the conservative threshold we used for designating a sample as a positive (Supplemental Tables 1A and 1B).

We did not observe an obvious independent effect of geography, year, or season on either the VirScan total EV enrichment or the ELISA VP1 EV data (Extended Data 3–5). To the extent

that the magnitude of CSF pleocytosis is a surrogate for the degree of inflammation and associated blood-brain barrier compromise, we found no correlation between the CSF cell count and the magnitude of EV antibodies as measured by either VirScan or VP1 ELISA (Extended Data 6A). Further, we found no relationship between the total CSF IgG concentration and the results of EV antibody testing by either VirScan or ELISA (Extended Data 6B). In addition, there was no difference observed in the total CSF IgG concentration between the subset of the AFM cases and OND controls for whom clinical laboratory data were available (Extended Data 6C). We did not observe a relationship between the input VirScan library and our immunoprecipitation results (Extended Data 7).

We attempted to identify serologic signatures specific to EV-A71 or EV-D68 using both VirScan and VP1 ELISA, but both assays yielded cross-reactivity in patients with known EV infections due to either EV-A71 or EV-D68 (Extended Data 8). Indeed, CSF from AFM cases were commonly enriched for antibodies targeting more than one EV species (Extended Data 9, Supplemental Tables 1A and 1B).

Discussion

We combined unbiased ultra-deep mNGS with an adaptation of the VirScan method for comprehensively detecting anti-viral antibodies to query CSF from a relatively large (n=42) and geographically diverse subset of children presenting with AFM since 2014.[19] Ultra-deep mNGS combined with FLASH enrichment for EV-A71 and EV-D68 confirmed the presence of EV RNA in a single sample that was previously known to be positive for EV-A71 by PCR and failed to discover any other pathogen in this or other AFM CSF samples. There are a number of possible reasons for the lack of detectable EV nucleic acid in the CSF of AFM patients by mNGS or other methods. Clinically, radiologically and similarly to poliomyelitis, the CNS tissue involved in AFM is often restricted to the anterior horn cells in the cervical spinal cord, making it possible that little to no virus is shed into the CSF. In addition, children with AFM, especially when associated with EV-D68, typically present with neurologic symptoms a median of 5–7 days after prodromal illness onset, decreasing the probability of RNA detection.[23]

Lack of consistent identification of viral nucleic acid in CSF is not limited to AFM, rather it is common to a wide range of neuroinvasive viruses, including poliovirus, rabies virus, West Nile virus, and other arboviruses.[24] As a result, detection of intrathecal antibody production through CSF serologic testing is the gold standard for diagnosis of many neuroinvasive viruses, notably West Nile virus and varicella-zoster virus.[25,26] Thus, we supplemented CSF mNGS with VirScan to comprehensively profile CSF anti-viral antibodies in AFM cases and OND controls. VirScan revealed high levels of CSF immunoreactivity to immunodominant EV epitopes in AFM, independent of whether EV RNA had previously been detected in clinical testing of CSF or nonsterile sites. There was a non-significant trend towards greater enrichment of EV antibodies in patients without directly detectable virus in a peripheral site, however, possibly owing to the rise in titer that occurs in the weeks following an infection. Independent testing with EV-A71 and EV-D68 VP1 ELISAs confirmed these findings. VirScan and whole VP1 ELISA were not able to consistently identify specific individual EV types, likely owing to cross-reactive immune responses to conserved linear EV antigens.[27]

Future studies using well-folded virus, rather than linear phage display peptides or individual viral proteins, may be more fruitful for identifying a species-specific serologic signature.

This study has important limitations. First, detection of a serologic response to a virus at a single time point by itself does not fulfill Koch's postulates for establishing causality between a virus and a particular disease. Nonetheless, these serologic data support the specificity of the CSF antibody response to EVs in AFM, helping fulfill the Bradford Hill criteria for making a causal association.[14,15] Second, further work will be necessary to establish, in a prospective manner, the diagnostic sensitivity and specificity for CSF EV serology. Third, our cases and controls were not optimally matched. While the controls had a diversity of pediatric ONDs, the case and control cohorts were not similar by age, year, or season, which are important risk factors for EV infection in the United States. However, we did not see a significant effect of year or season on EV signal by VirScan or ELISA in the OND controls. We chose to report these preliminary findings, despite the limitations of the study design, because of the public health urgency of understanding the etiology of AFM. A prospective study with matched cases and controls is necessary to confirm our findings.

AFM is a potentially devastating neurologic syndrome whose incidence of reported cases has risen in the US since 2014 with biennial peaks. In addition, cases have now been detected in 14 other countries across 6 continents.[23] There are no proven treatments for AFM, and like poliomyelitis, a vaccine may ultimately be the most effective prevention strategy. However, it is important to first achieve consensus around the likely etiologic agents. While continued vigilance for other possible etiologies of AFM is warranted, together our combined mNGS, VirScan, and viral protein ELISA interrogation of AFM CSF supports the notion that EV infection likely underlies the majority of AFM cases tested in this study. These results offer a roadmap for rapid development of EV CSF antibody assays to enable efficient clinical diagnosis of EV-associated AFM in the future.

Methods

Detailed methods for data collection, human subjects review, mNGS, VirScan, bioinformatics, and independent confirmatory testing with ELISA are provided in the Supplemental Appendix.

Case-Control Design

All AFM cases met the 2018 US Council of State and Territorial Epidemiologists case definition for probable or confirmed AFM (Supplemental Table 7).[28] Patient samples were collected with informed consent either through enrollment in research studies or through public health surveillance. In addition, residual banked CSF was obtained from children with other neurologic diseases (ONDs) without suspected primary EV infection and without known exposure to intravenous gamma globulin for controls.

Metagenomic Sequencing Library Preparation

CSF was shipped on dry ice to our laboratory and stored immediately upon receipt at −80°C until use. RNA sequencing libraries were prepared using a previously described protocol

optimized and adapted for miniaturization and automation.[29] Libraries were sequenced on a NovaSeq 6000 machine (Illumina) to generate 150 nucleotide (nt), paired-end reads. Samples were also sequenced after enrichment for EV-A71 and EV-D68 genomes using FLASH (Finding Low Abundance Sequences by Hybridization, Supplemental Table 2).[18] All NGS libraries were depleted of host ribosomal RNA with DASH (Depletion of Abundant Sequences by Hybridization) and spiked-in with External RNA Controls Consortium (ERCC) sequences as previously described.[20,30]

Metagenomic Bioinformatics

As previously described, pathogens were identified from raw mNGS sequencing reads using IDseq v3.2, a cloud-based, open-source bioinformatics platform designed for detection of microbes from mNGS data.[31]

Pan-Viral CSF Serologic Testing with VirScan

The previously published VirScan method is an application of programmable phage immunoprecipitation-sequencing (PhIP-Seq), displaying viral peptides on the outer surface of bacteriophage for the purposes of antibody detection followed by deep sequencing.[19,32] Similarly, we constructed a T7 bacteriophage display library comprised of 481,966 sixty-two amino acid peptides with a 14 amino acid overlap tiled across a representative set of full-length, vertebrate, mosquito-borne, and tick-borne viral genomes downloaded from the UniProt and RefSeq databases in February 2017 (Supplemental Table 8A–D). After amplification, phage libraries were incubated with 2 μL of patient CSF overnight and then immunoprecipitated for two rounds as previously described.[33,34] Barcoded phage DNA was sequenced on a HiSeq 4000 machine (Illumina) using 150 nt paired-end reads.

VirScan Bioinformatics

Sequencing reads were aligned to a reference database comprising the full viral peptide library. Peptide counts were normalized by dividing by the sum of counts and multiplying by 100,000 (reads per hundred thousand (rpK)).[33–36] Phage rpK results for each phage in each subject were filtered using a cutoff fold-change of greater than 10 above the mean background rpK generated from null IPs (Supplemental Table 9). A sample was considered EV positive if the total EV rpK value was greater than the mean signal in the OND controls plus one standard deviation.

Independent Validation with ELISA

To independently validate our VirScan results, we generated recombinant viral protein 1 (VP1) from recent AFM-associated EV-A71 and EV-D68 strains and performed ELISA to detect EV antibodies with AFM CSF samples for which sufficient CSF remained (n=26) and OND controls (n=50). Signal was measured as the optical density (OD) at 450 nm and reported after background subtraction (background OD = 0.05). For each sample, we considered the higher of the two (EV-A71 or EV-D68) OD values when analyzing cases and controls. A sample was considered positive if the reported OD was greater than three times the background.

Statistical Methods

VirScan data comparisons between AFM cases and OND controls were made using the Mann-Whitney test with Bonferroni adjustment for multiple comparisons, n=42 AFM cases and n=58 OND controls. EV VP1 signal by ELISA was compared between n=26 AFM cases and n=50 OND controls using the Mann-Whitney test. When subsets were tested, exact n and statistical tests are provided in figure legends. All error bars are defined in figure legends.

Data Availability Statement—VirScan and clinical data analyzed in the manuscript have been made available in the online supplementary material. The non-human sequence reads from the mNGS experiments for each sample were deposited at the National Center for Biotechnology Information Sequence Read Archive (PRJNA557094).

Extended Data

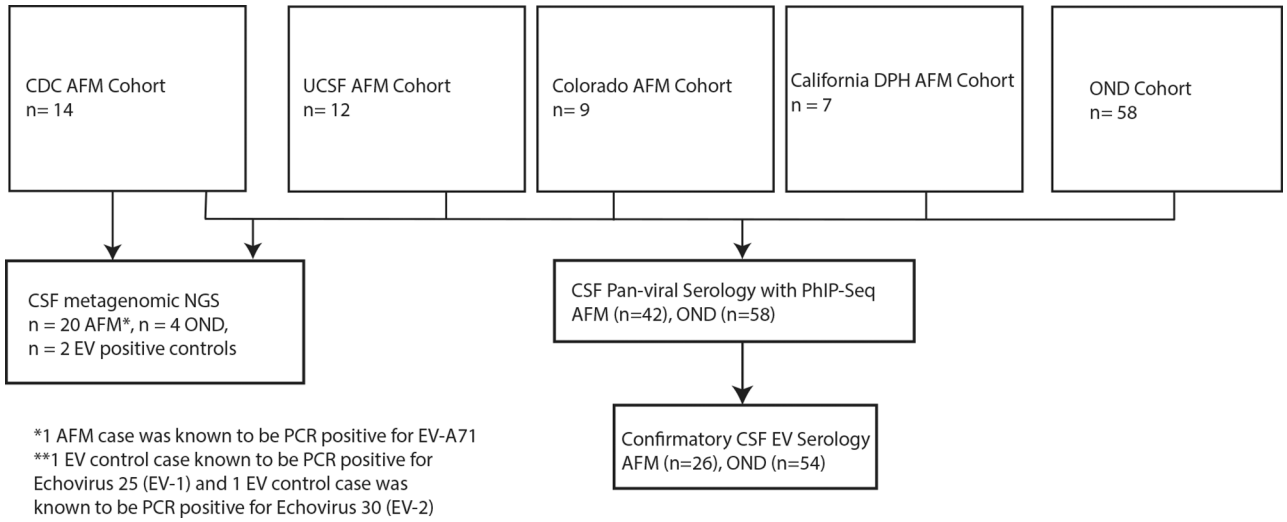

Extended Data Fig. 1. Flow chart depicting patient enrollment by institution

mNGS with and without FLASH were performed on CSF samples acquired from the CDC (n=14 AFM, n=4 OND, n=2 EV positive controls) and UCSF AFM Cohort (n=6 AFM). Samples from all institutions were tested by VirScan. Due to limited sample, a subset of those tested by VirScan were tested by confirmatory ELISA.

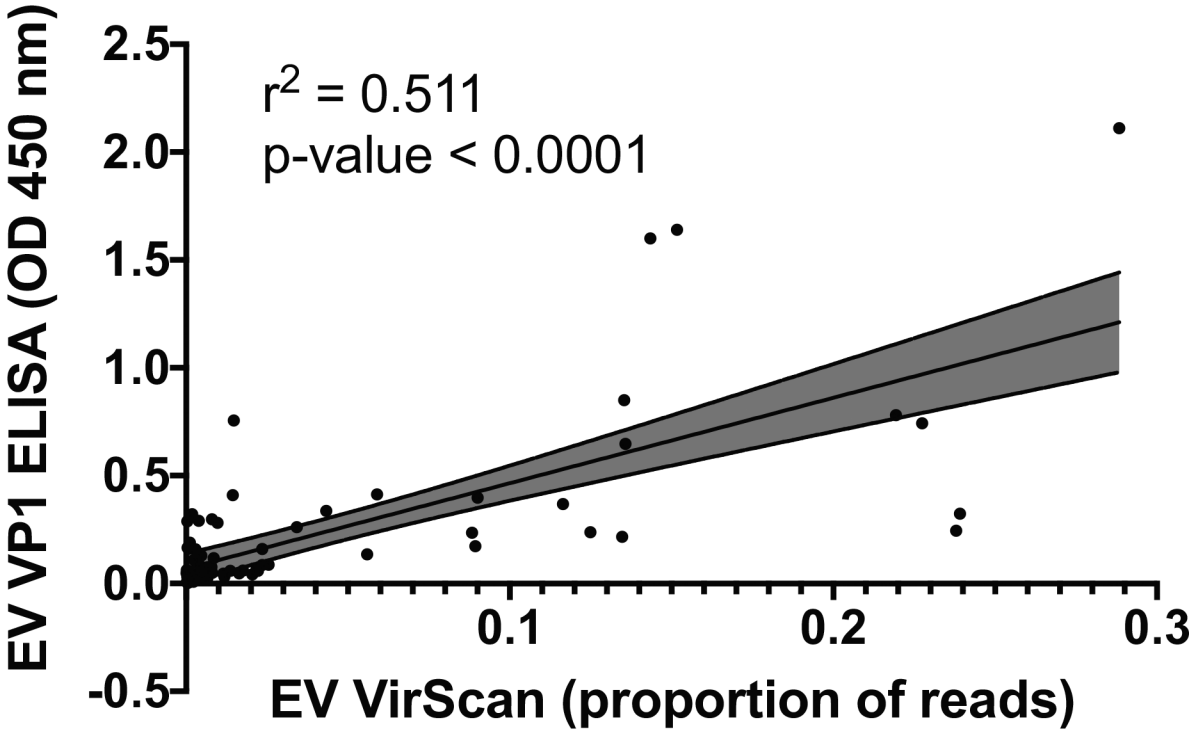

Extended Data Fig. 2. Comparison of VirScan and ELISA

A comparison of the total amount of enterovirus signal generated by VirScan (x-axis) to the maximum OD generated by either EV-D68 or EV-A71 signal ELISA (greater of the two values shown) for all samples run (n = 26 AFM + 50 OND). The 95% confidence intervals are shaded in grey.

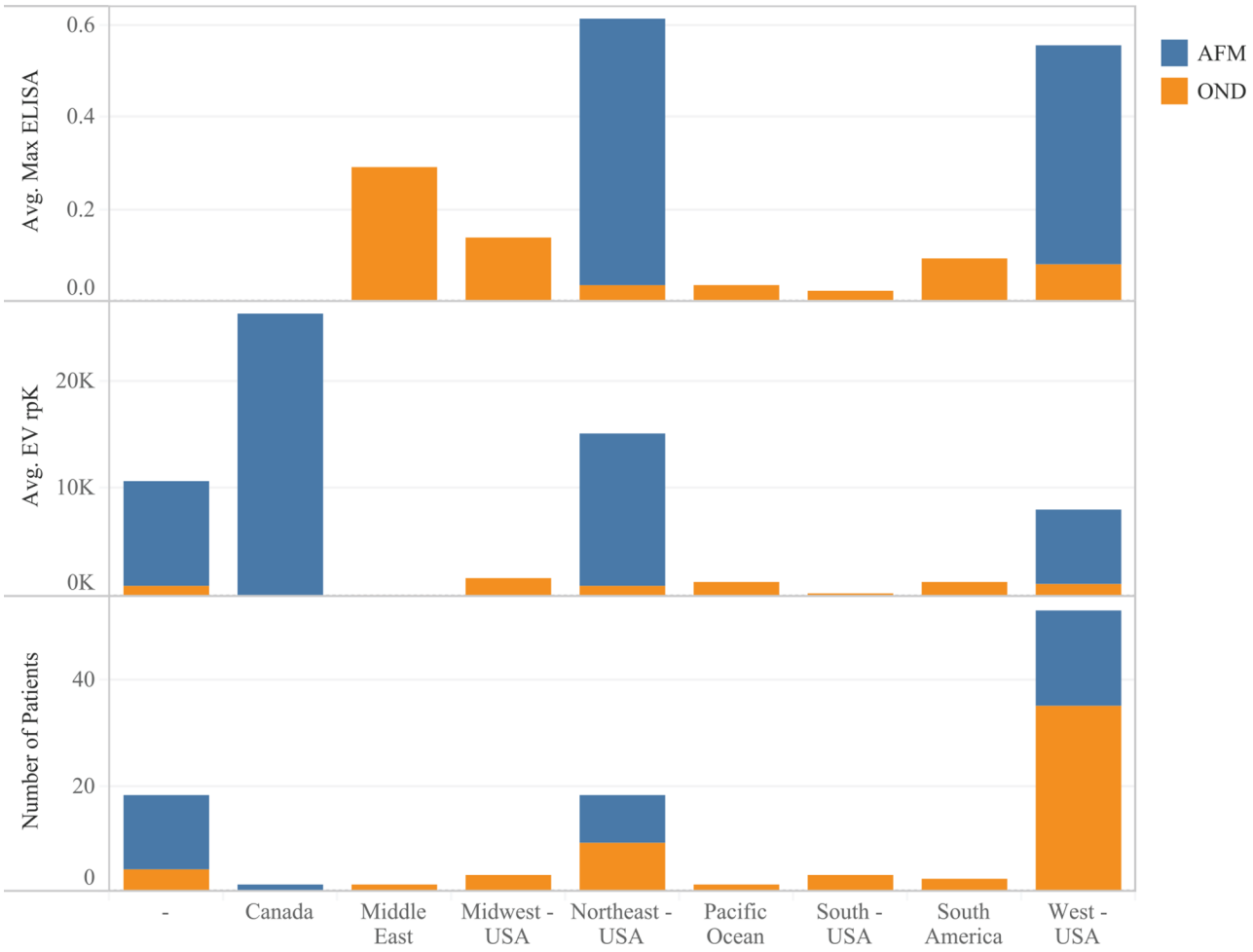

Extended Data Fig. 3. Geographic distribution of cases and controls

Geographic comparison of cases (blue) and controls (orange) with average EV signal by ELISA (top), average EV signal by VirScan (middle), and total number (bottom).

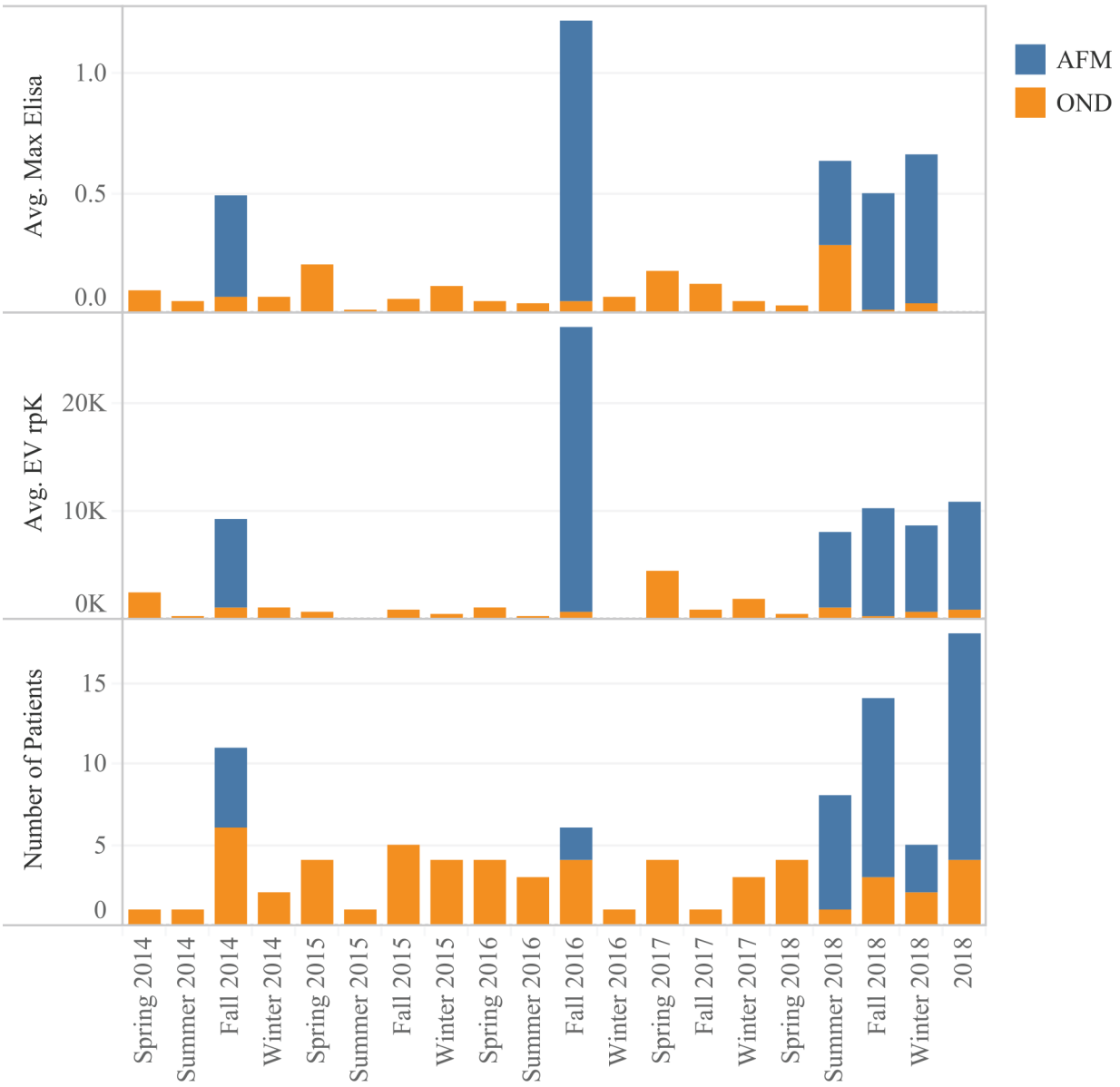

Extended Data Fig. 4. Season and year of cases and controls

Season and year comparison for cases (blue) and controls (orange) with average EV signal by ELISA (top), average EV signal by VirScan (middle), and total number (bottom).

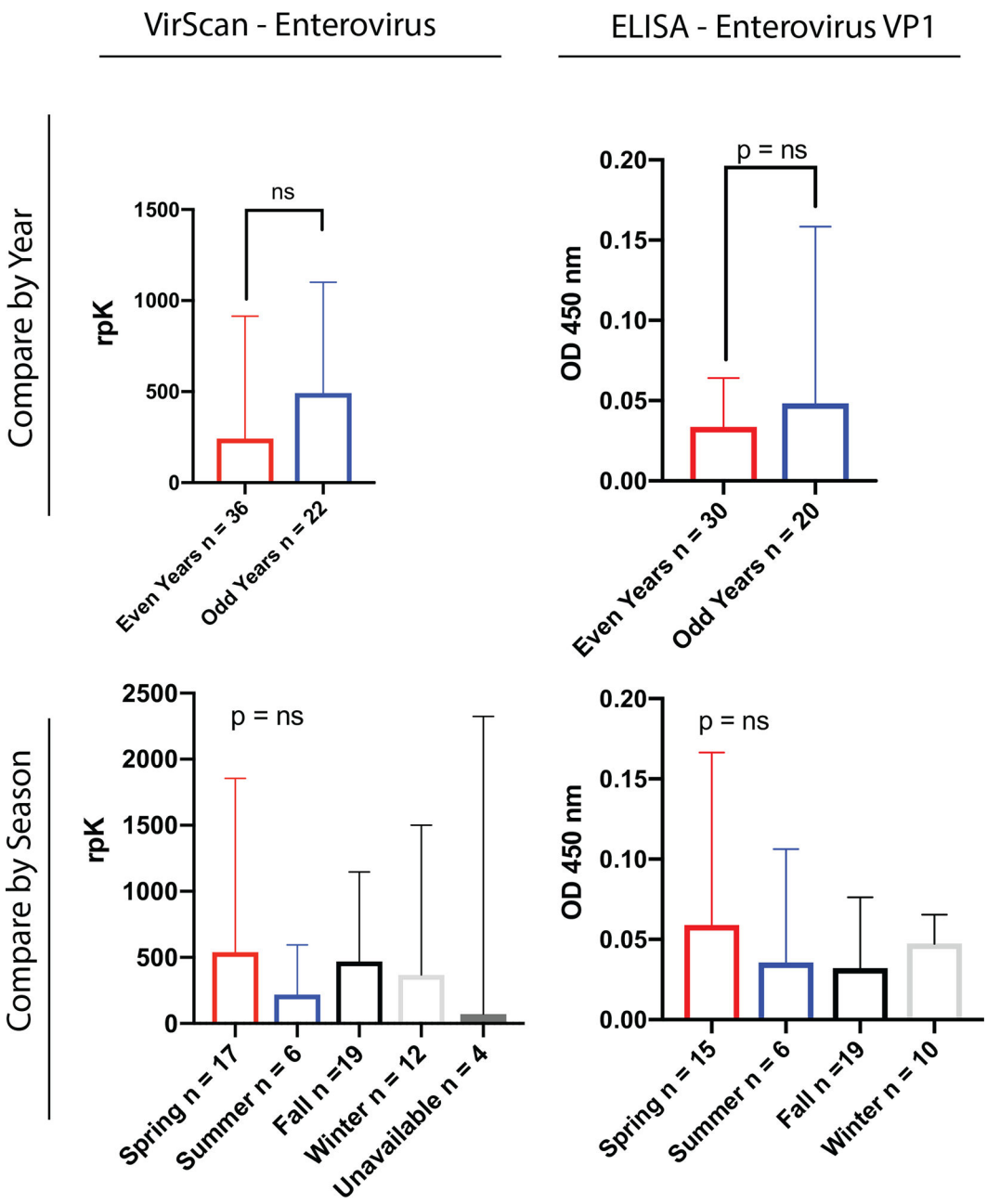

Extended Data Fig. 5. Analysis of effect of year and season on enterovirus signal in the OND controls.

EV VirScan (left, n = 54) and EV VP1 ELISA (right, n = 50) for the OND control cohort by year (top) and season (bottom). Bar graphs depict heights as median values with error bars reflecting the interquartile range. Statistics for year were performed with the Mann-Whitney test and for seasons with the Kruskal-Wallis test.

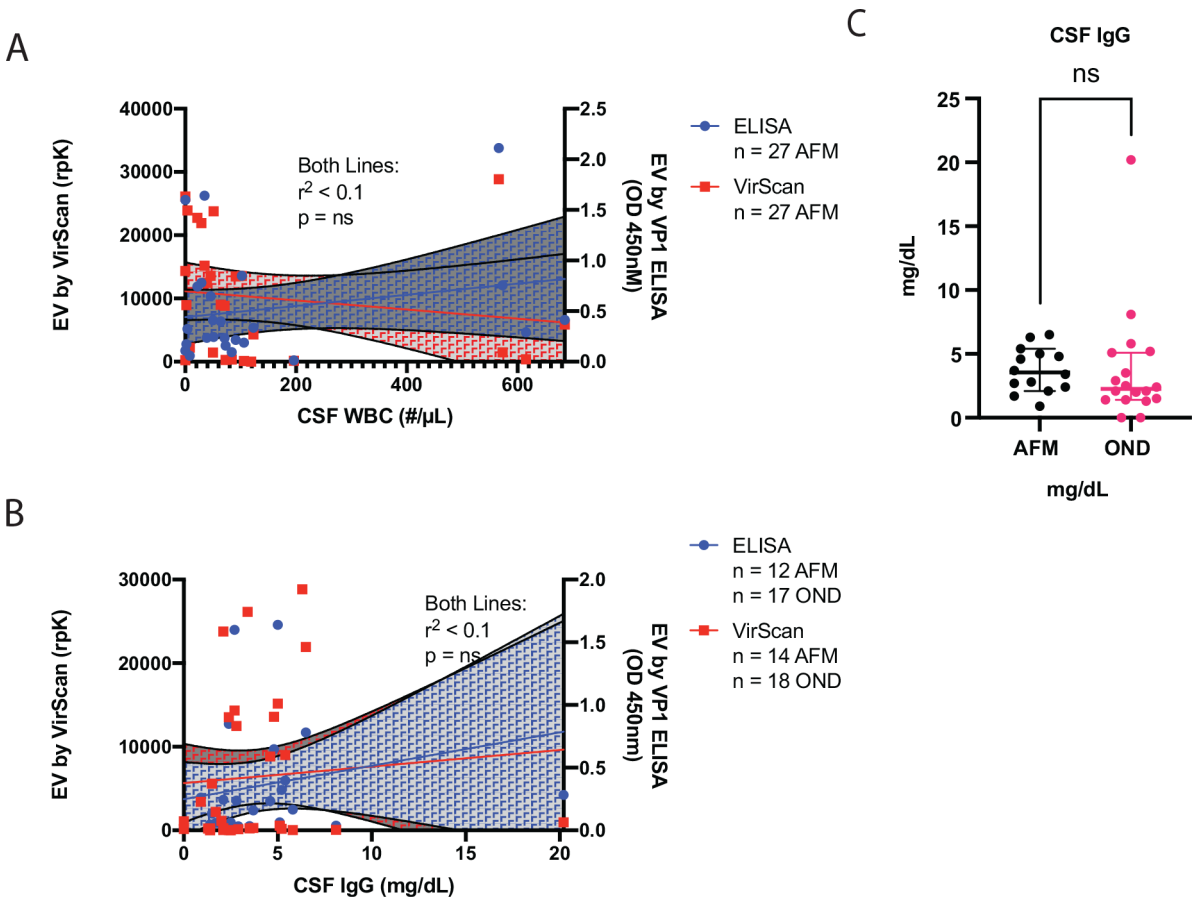

Extended Data Fig. 6. CSF cell count and IgG concentration in cases and controls do not explain EV signal by VirScan or ELISA.

CSF enterovirus antibodies by VirScan a and ELISA are not correlated with the overall amount of CNS inflammation as measured by the CSF cell count (panel A) or CSF IgG (panel B) in a subset of patients. The 95% confidence intervals for each measurement are shaded in blue (ELISA) or red (Virscan). When comparing the concentration of IgG in a subset of AFM cases and OND controls, there was no difference in CSF IgG concentration (p = ns by Mann-Whitney, mean with errors bars showing standard deviation displayed). Two OND CSF IgG values were reported as < 0.9 mg/dL and were conservatively estimated to be 0. Errors bars represent 95% confidence intervals.

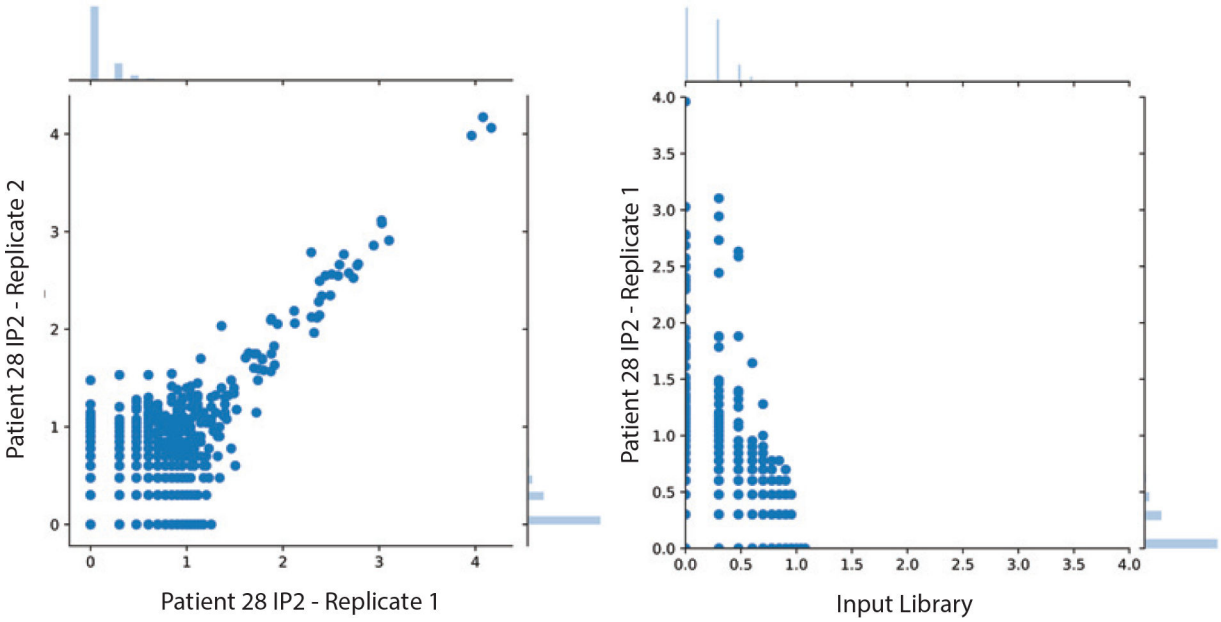

Extended Data Fig. 7. Enterovirus antibody enrichment in AFM cases with VirScan is not a reflection of bias in the input library.

Dotplot demonstrating replicate IPs from a typical sample (left panel) correlate with each other but not with the input library (right panel). Values plotted are log10 of the raw rpK values + 1. The sum of the signal at each point on the axes is expressed as a barplot on the axes of the graph.

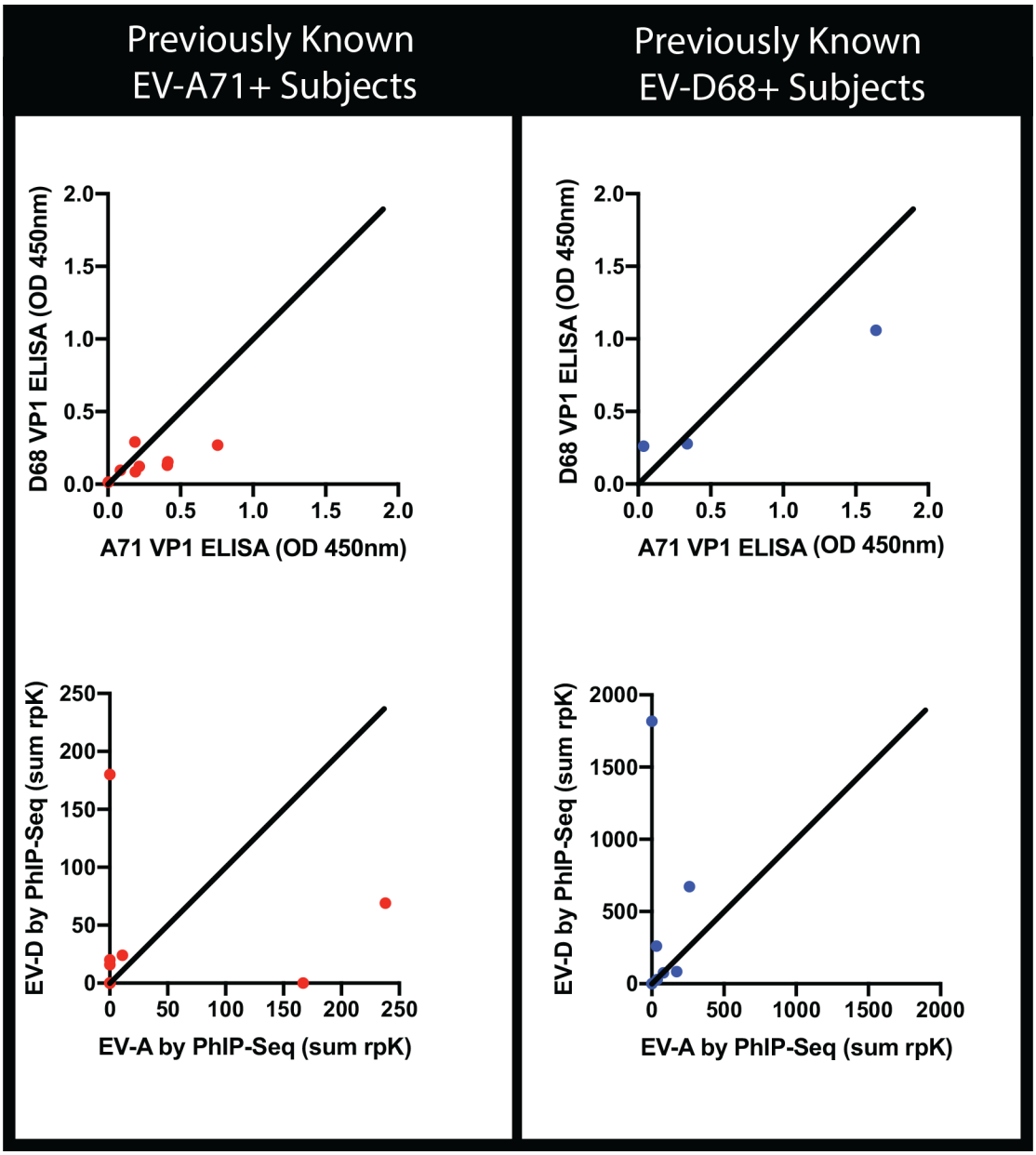

Extended Data Fig. 8. Strain calling by ELISA versus VirScan

ELISA and VirScan data from subjects with EV-A71 or EV-D68 detected by RT-PCR in either CSF, stool or respiratory fluid. Top panels with strain-specific VP1 ELISA data from EV-A71 (n = 8, red) and EV-D68 (n = 3, blue) patients show cross reactivity. Bottom panels shows VirScan data from known EV-A71 (n = 9, red) and EV-D68 (n = 7, blue) patients. EV-A and EV-D signals were generated by summing the total rpK generated against EV-A and EV-D derived peptides within a sample.

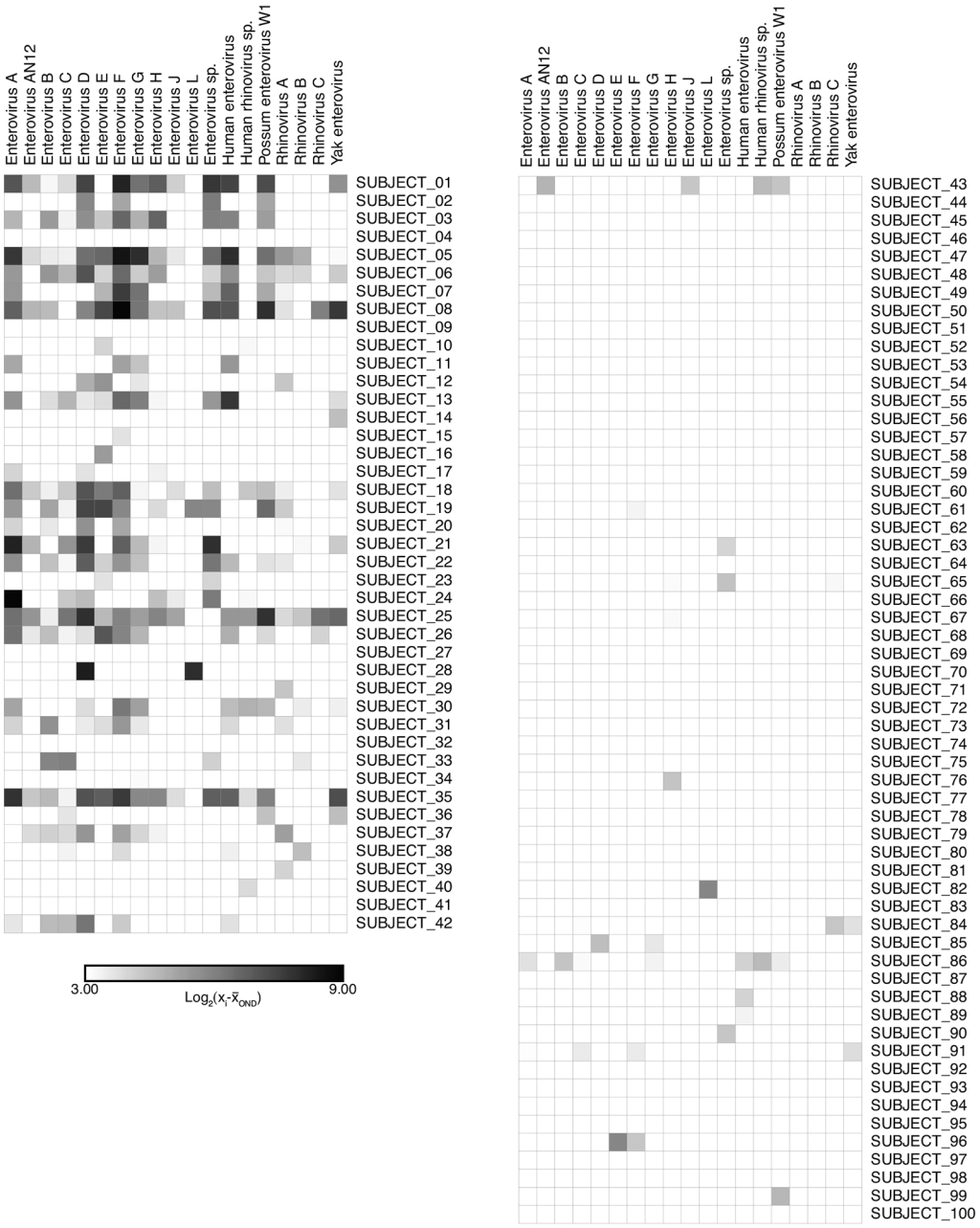

Extended Data Fig. 9. Enterovirus species per-subject heatmap.

VirScan enterovirus genus signal in each subject demonstrating enrichment for a cross-reactive EV signal in the AFM subjects (left) as compared with OND (right). Signal represents the log base 2 of the subject's EV rpK value divided by the mean rpK value in the OND subjects for each EV species. To increase clarity, resulting values below 3 are not shown (legend).

Supplementary Material

Refer to Web version on PubMed Central for supplementary material.

Acknowledgments

This work is supported by a National Multiple Sclerosis Society-American Brain Foundation Clinician Scientist Development Award FAN-1608–25607 (R.D.S.), UCSF Biomedical Sciences Graduate Program (I.A.H.), American Academy of Neurology Clinical Research Training Scholarship P0534134 (P.S.R.), UCSF Dean's Office Medical Student Research Program (G.A.S.), UCSF Bioinformatics Graduate Program (B.O.), NIH grants K08NS096117 (M.R.W.) and K23AI28069 (K.M.), the Chan Zuckerberg Biohub (J.L.D., C.M.T., J.E.P., E.D.C., W.W., C.K.C., A.L., M.T., R.S.), an endowment from the Rachleff family (M.R.W.), and the Sandler and William K. Bowes, Jr. Foundations (M.R.W., K.C.Z., H.A.S., C.Y.C., L.M.K., B.O., and J.L.D.). We thank Herb Sandler, William Bowes, Jr., and Debbie and Andy Rachleff for their encouragement. We would like to thank the patients and their families for their participation in this study.

References:

1. Sejvar JJ, et al. Acute Flaccid Myelitis in the United States, August-December 2014: Results of Nationwide Surveillance. Clinical infectious diseases: an official publication of the Infectious Diseases Society of America 63, 737–745 (2016). [PubMed: 27318332]
2. Van Haren K, et al. Acute Flaccid Myelitis of Unknown Etiology in California, 2012–2015. JAMA 314, 2663–2671 (2015). [PubMed: 26720027]
3. Greninger AL, et al. A novel outbreak enterovirus D68 strain associated with acute flaccid myelitis cases in the USA (2012–14): a retrospective cohort study. The Lancet. Infectious diseases 15, 671–682 (2015). [PubMed: 25837569]
4. McKay SL, et al. Increase in Acute Flaccid Myelitis - United States, 2018. MMWR Morb Mortal Wkly Rep 67, 1273–1275 (2018). [PubMed: 30439867]
5. CDC AFM Confirmed U.S. Cases To Date. (2019).
6. Messacar K, Pretty K, Reno S & Dominguez SR Continued biennial circulation of enterovirus D68 in Colorado. J Clin Virol 113, 24–26 (2019). [PubMed: 30825833]
7. Ayscue P, et al. Acute flaccid paralysis with anterior myelitis - California, June 2012-June 2014. MMWR Morb Mortal Wkly Rep 63, 903–906 (2014). [PubMed: 25299608]
8. Pruss H, et al. N-methyl-D-aspartate receptor antibodies in herpes simplex encephalitis. Annals of neurology 72, 902–911 (2012). [PubMed: 23280840]
9. Aliabadi N, et al. Enterovirus D68 Infection in Children with Acute Flaccid Myelitis, Colorado, USA, 2014. Emerging infectious diseases 22, 1387–1394 (2016). [PubMed: 27434186]
10. Iverson SA, et al. Notes from the Field: Cluster of Acute Flaccid Myelitis in Five Pediatric Patients - Maricopa County, Arizona, 2016. MMWR Morb Mortal Wkly Rep 66, 758–760 (2017). [PubMed: 28727681]
11. Messacar K, et al. Notes from the Field: Enterovirus A71 Neurologic Disease in Children - Colorado, 2018. MMWR Morb Mortal Wkly Rep 67, 1017–1018 (2018). [PubMed: 30212441]
12. Jubelt B & Lipton HL Enterovirus/picornavirus infections. Handb Clin Neurol 123, 379–416 (2014). [PubMed: 25015496]
13. Hixon AM, et al. A mouse model of paralytic myelitis caused by enterovirus D68. PLoS pathogens 13, e1006199 (2017). [PubMed: 28231269]
14. Dyda A, Stelzer-Braid S, Adam D, Chughtai AA & MacIntyre CR The association between acute flaccid myelitis (AFM) and Enterovirus D68 (EV-D68) - what is the evidence for causation? Euro Surveill 23(2018).
15. Messacar K, et al. Enterovirus D68 and acute flaccid myelitis-evaluating the evidence for causality. Lancet Infect Dis 18, e239–e247 (2018). [PubMed: 29482893]
16. Messacar K, et al. Acute flaccid myelitis: A clinical review of US cases 2012–2015. Ann Neurol 80, 326–338 (2016). [PubMed: 27422805]
17. Moline H, et al. Notes from the Field: Six Cases of Acute Flaccid Myelitis in Children - Minnesota, 2018. MMWR Morb Mortal Wkly Rep 68, 356–358 (2019). [PubMed: 30998669]
18. Quan J, et al. FLASH: a next-generation CRISPR diagnostic for multiplexed detection of antimicrobial resistance sequences. Nucleic Acids Res 47, e83 (2019). [PubMed: 31114866]
19. Xu GJ, et al. Viral immunology. Comprehensive serological profiling of human populations using a synthetic human virome. Science 348, aaa0698 (2015). [PubMed: 26045439]

20. Baker SC, et al. The External RNA Controls Consortium: a progress report. Nat Methods 2, 731–734 (2005). [PubMed: 16179916]
21. Gao F, et al. Enterovirus 71 viral capsid protein linear epitopes: identification and characterization. Virol J 9, 26 (2012). [PubMed: 22264266]
22. Mishra N, et al. Antibodies to Enteroviruses in Cerebrospinal Fluid of Patients with Acute Flaccid Myelitis. MBio 10(2019).
23. Messacar K & Tyler KL Enterovirus D68-Associated Acute Flaccid Myelitis: Rising to the Clinical and Research Challenges. JAMA (2019).
24. Ramachandran PS & Wilson MR Diagnostic Testing of Neurologic Infections. Neurologic clinics 36, 687–703 (2018). [PubMed: 30366549]
25. Gilden D, Cohrs RJ, Mahalingam R & Nagel MA Varicella zoster virus vasculopathies: diverse clinical manifestations, laboratory features, pathogenesis, and treatment. Lancet Neurol 8, 731–740 (2009). [PubMed: 19608099]
26. Chabierski S, et al. Distinguishing West Nile virus infection using a recombinant envelope protein with mutations in the conserved fusion-loop. BMC Infect Dis 14, 246 (2014). [PubMed: 24884467]
27. Samuelson A, Forsgren M, Johansson B, Wahren B & Sallberg M Molecular basis for serological cross-reactivity between enteroviruses. Clin Diagn Lab Immunol 1, 336–341 (1994). [PubMed: 7496972]
28. Council of State and Territorial Epidemiologists. Revision to the Standardized Surveillance and Case Definition for Acute Flaccid Myelitis. https://cdn.ymaws.com/www.cste.org/resource/resmgr/2017ps/2017psfinal/17-ID-01.pdf Published 2018. Accessed April 2019.
29. Mayday MY, Khan LM, Chow ED, Zinter MS & DeRisi JL Miniaturization and optimization of 384-well compatible RNA sequencing library preparation. PloS one 14, e0206194 (2019). [PubMed: 30629604]
30. Gu W, et al. Depletion of Abundant Sequences by Hybridization (DASH): using Cas9 to remove unwanted high-abundance species in sequencing libraries and molecular counting applications. Genome Biol 17, 41 (2016). [PubMed: 26944702]
31. Ramesh A, et al. Metagenomic next-generation sequencing of samples from pediatric febrile illness in Tororo, Uganda. PLoS One 14, e0218318 (2019). [PubMed: 31220115]
32. Pou C, et al. The repertoire of maternal anti-viral antibodies in human newborns. Nat Med 25, 591–596 (2019). [PubMed: 30886409]
33. O'Donovan B, Mandel-Brehm C, Vazquez SE, et al. Exploration of Anti-Yo and Anti-Hu paraneoplastic neurological disorders by PhIP-Seq reveals a highly restricted pattern of antibody epitopes. Biorxiv (2018).
34. Mandel-Brehm C, et al. Kelch-like Protein 11 Antibodies in Seminoma-Associated Paraneoplastic Encephalitis. N Engl J Med 381, 47–54 (2019). [PubMed: 31269365]
35. Zhang J, Kobert K, Flouri T & Stamatakis A PEAR: a fast and accurate Illumina Paired-End reAd mergeR. Bioinformatics 30, 614–620 (2014). [PubMed: 24142950]
36. Langmead B & Salzberg SL Fast gapped-read alignment with Bowtie 2. Nat Methods 9, 357–359 (2012). [PubMed: 22388286]

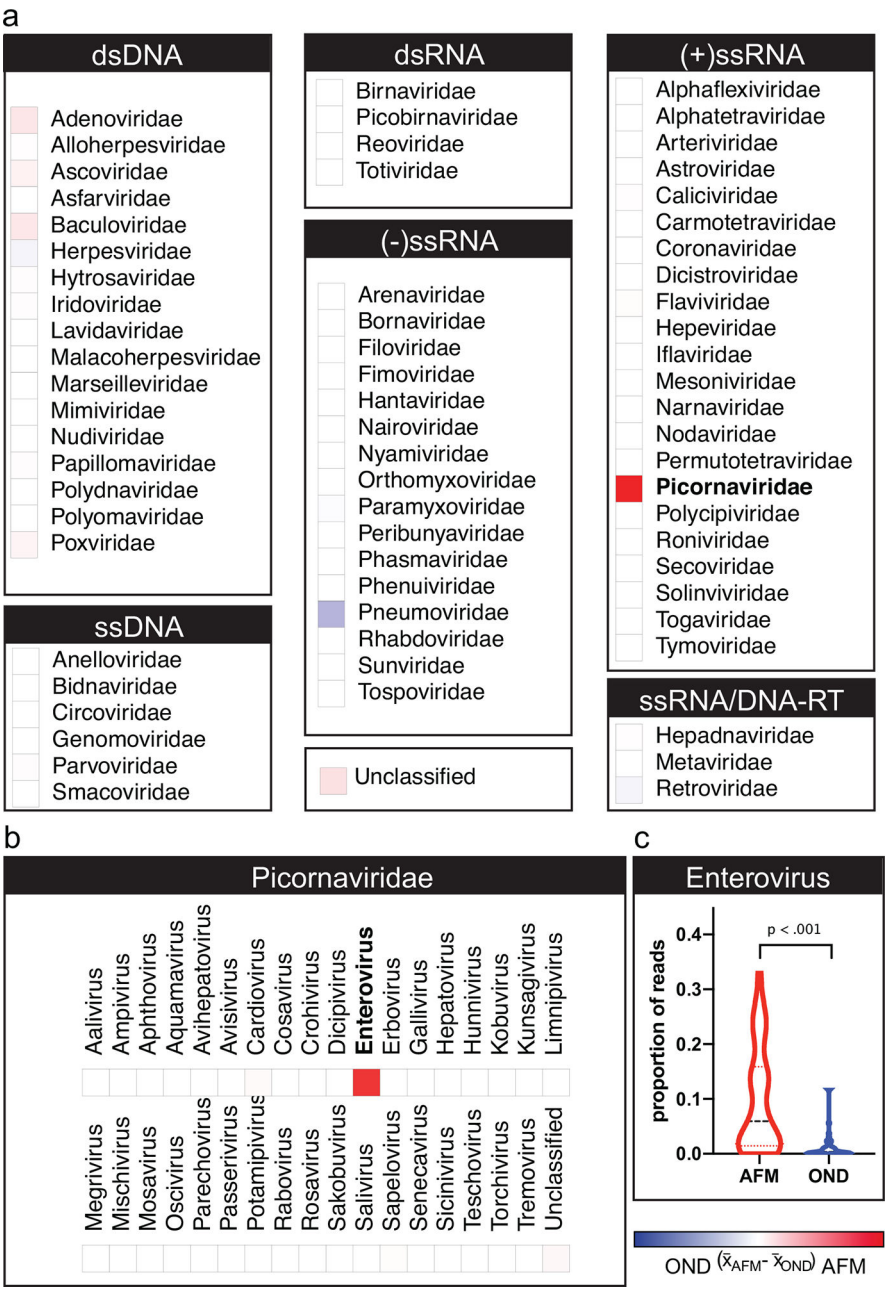

Figure 1. Enterovirus Immunoreactivity in Acute Flaccid Myelitis on a Pan-Viral Phage Display Assay.

(A) Viral families detected by VirScan or phage display immunoprecipitation with next-generation sequencing (PhIP-Seq) sorted by their Baltimore classification. Heatmap color intensity was calculated by subtracting the mean reads per hundred thousand sequenced (rpK) in the other neurologic disease (OND) cerebrospinal fluid sample set (n=58) from that observed in acute flaccid myelitis (AFM) CSF (n=42). The maximum and minimum color intensities reflect +11,000 and −11,000 rpK, respectively. The strongest intensity is observed in the *Picornaviridae* family (boldface type). **(B)** Genus *Enterovirus* demonstrating the strongest enrichment in family *Picornaviridae*. **(C)** Violin plot of the proportion of

Enterovirus phage per patient with mean and first and third quartile indicated by horizontal lines; Mann-Whitney test corrected for multiple comparisons with a Bonferroni adjustment.

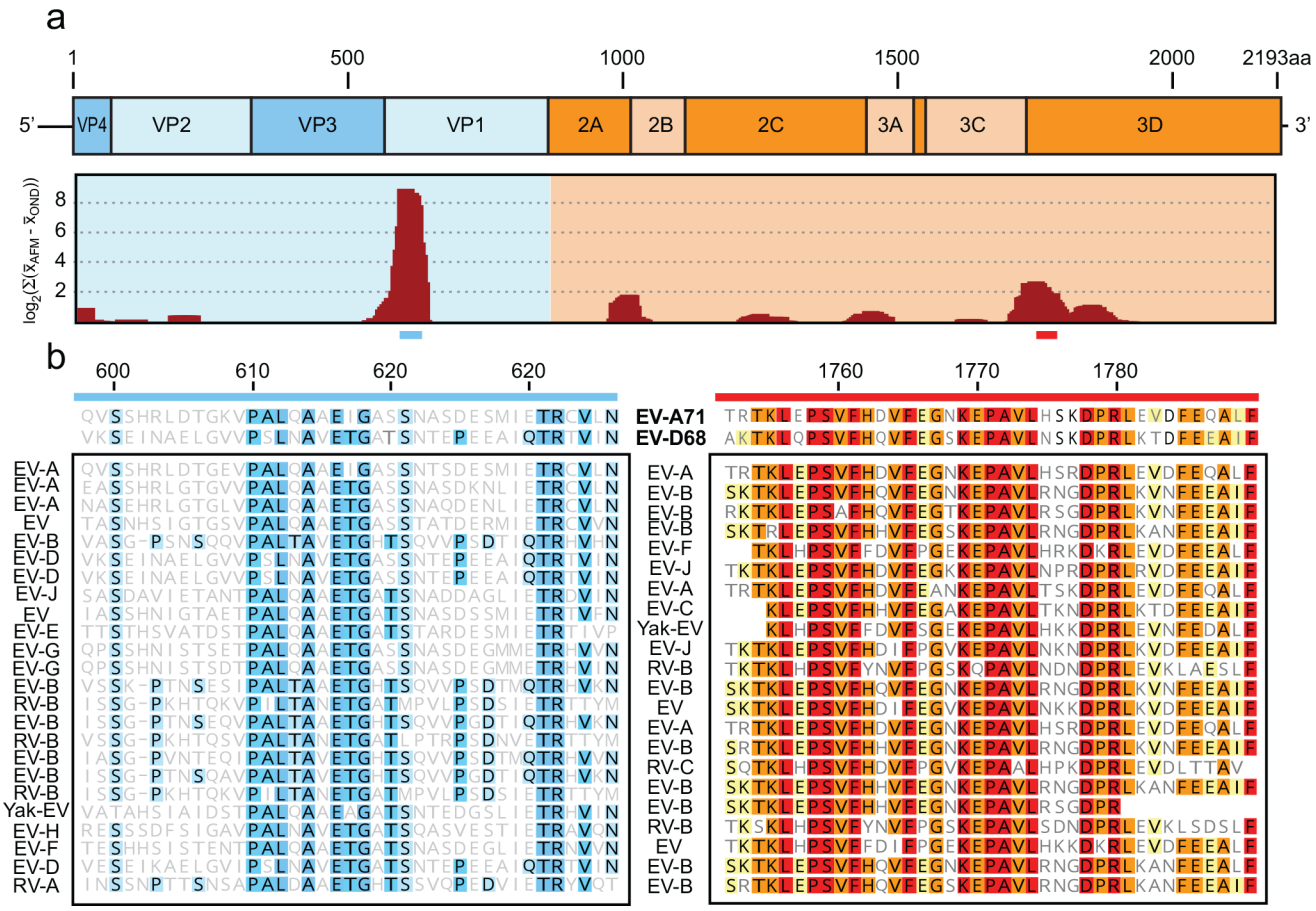

Figure 2. Primary Enterovirus Antigens Identified by Pan-Viral Phage Display in Acute Flaccid Myelitis.

We identified 438 unique, enriched antigens with taxonomic identifications mapping to enterovirus (EV) across all acute flaccid myelitis (AFM) cerebrospinal fluid samples (n=42). **(A)** 420 of 438 EV derived peptides were mapped by BLASTP to the 2,193 amino acid polyprotein of EV-A71 (Genbank Accession AXK59213.1) as a model reference. The relative recovery of these peptides by VirScan is plotted as the $\log_2$ of the sum of the differences in the mean signal generated in the AFM and pediatric other neurologic disease (OND) cohorts, using a moving average of 32 amino acids, advanced by 4 amino acid steps. **(B)** Multiple sequence alignment of a representative set of enriched EV-derived peptides for the VP1 (blue bar) and 3D (red bar) proteins. Sequences from EV-D68 (Genbank Accession AIT52326.1) and EV-A71 (Genbank Accession AXK59213.1) are included for reference. Amino acids are shaded to indicate shared identity among peptides from the indicated EV species.

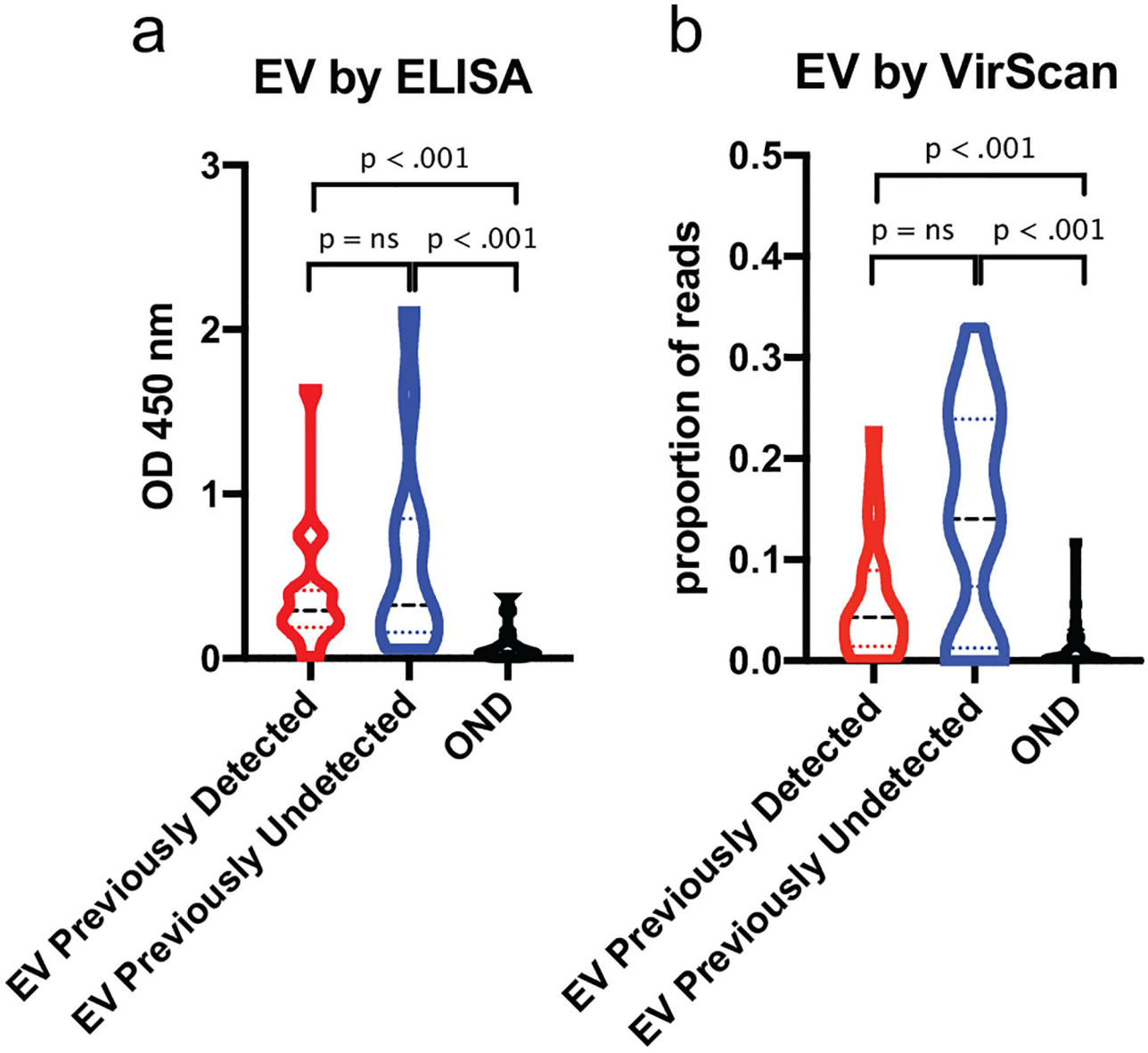

Figure 3. Independent Validation of Pan-Viral Phage Display with Purified Enterovirus VP1 Capsid Protein.

(A) Violin plot that enterovirus (EV) signal generated by ELISA can be found at similar levels in acute flaccid myelitis (AFM) patients with previously detected (n=15) and previously undetected (n=11) EV infections (p = ns). In both AFM cohorts, there was a significantly greater amount of signal generated by ELISA compared with pediatric other neurologic disease (OND) controls (n=50) ($p < 0.001$ for both comparisons, Mann-Whitney test). (B) Similar results by VirScan with no differences seen when comparing EV signal in AFM patients with previously detected (n=23) and previously undetected (n=19) EV infections (p = ns). When each group was compared to the OND controls (n=58), both demonstrated significant enrichment of EV signal ($p < 0.001$; Mann-Whitney test with Bonferroni adjustment for multiple comparisons).

Table 1.

Characteristics of the Patients at Baseline

	AFM Cases	OND Controls
N	42	58
Age – median (IQR), months	38 (11 to 64)	120 (66–174)
Sex – no. (%)		
Female	13 (31)	32 (55)
Male	29 (69)	26 (45)
Region – no. (%)		
United States		
West	20 (48)	37 (64)
South	7 (17)	4 (7)
Midwest	3 (7)	4 (7)
Northeast	11 (26)	9 (16)
International		
South America	0 (0)	2 (3)
Canada	1 (2)	0 (0)
North Atlantic Island	0 (0)	1 (2)
Middle East	0 (0)	1 (2)
Year – no. (%)		
2014	5 (12)	10 (17)
2015	0 (0)	14 (24)
2016	2 (5)	12 (21)
2017	0 (0)	8 (14)
2018	34 (81)	14 (24)
Season – no. (%)		
Spring	1 (2)	18 (31)
Summer	12 (29)	8 (14)
Fall	24 (57)	20 (34)
Winter	5 (12)	12 (21)
Suspected Etiology – no. (%)		
Infectious	-	23 (40)
Autoimmune	-	22 (38)
Non-inflammatory	-	6 (10)
Malignancy	-	3 (5)
Unavailable	-	4 (7)

NB: Percentages may not total 100 because of rounding.